DOI: 10.1002/chem.200601813

Organogels of 8-Quinolinol/Metal(II)–Chelate Derivatives That Show Electron- and Light-Emitting Properties

Michihiro Shirakawa,[a] Norifumi Fujita,[a] Takahiro Tani,[a] Kenji Kaneko,[b] Masayoshi Ojima,[c] Akihiko Fujii,[c] Masanori Ozaki,[c] and Seiji Shinkai*[a, d]

Abstract: 8-Quinolinol/copper(II)-, palladium(II)-, and platinum(II)-chelate-based organogelators (**1M**) and their nongelling reference compounds (**2M**) were synthesized. Complexes **1M** could gelate various organic solvents at very low concentrations. Electron microscope measurements gave visual images of well-developed fibrous structures characteristic of low-molecular-weight organogels. UV/Vis and FTIR spectroscopy revealed that the good gelation ability of **1M** arises from the π–π interactions of the chelate moieties and the hydrogen-bond interactions among the amide groups. Very interestingly, field emission performances of the nanofibers prepared from the **1M** gels are evidently different depending on the electronic states of the three kinds of central metals. In addition, the **1Pt** gel shows unique thermo- and solvatochromism of visible and phosphorescent color in response to a sol–gel phase transition. Furthermore, the **1Pt** gel possesses an attractive ability to inhibit dioxygen quenching of excited triplet states, which increases the phosphorescence quantum yield of this gel. This effect is attributed to the isolation effect of the phosphorescent chelate moiety from the dioxygen-containing solution phase.

Keywords: chelates · field emission · gels · phosphorescence · self-assembly

Introduction

Spontaneous, but programmed self-assembly of low-molecular-weight compounds is an essential concept to construct distinct supramolecules for nanotechnology by the bottom-up method. Among various supramolecular architectures developed thus far, low-molecular-weight gel systems have become a topic of growing interest because they are expected to be useful not only as novel functional soft materials, but also as well-defined nanostructured assemblies.[1] In particular, π-block-based low-molecular-weight gels have received much attention, because they have great potential in applications for nanoscale molecular electronics.[2,3]

In the last several years, low-molecular-weight organogels with metal–chelate moieties, namely metallogels, have been widely investigated to explore advanced soft and nanomaterials.[4] Metal chelates are favorable from a viewpoint of gel functionality because they have not only various electronic states arising from inorganic metal elements, but also limitless possibilities of molecular design arising from organic ligands. Until now, metallogels with various features of metal chelates have been reported to show unusual functional properties such as redox responsiveness,[5] catalytic action,[6] phosphorescence behavior,[7] spin-crossover phenomena,[8] conductivities,[9] and so on.[10] Among the numerous metal chelates, 8-quinolinol/metal–chelate derivatives are known to possess attractive electronic and luminescent properties. For instance, tri(8-quinolinol)aluminum (Alq_3) has become one of the most efficient electron transport and emitting materials for organic light-emitting diode devices.[11] Furthermore, Alq_3 nanowires and nanobelts are utilized as field emission materials.[12]

Here, we report on gel formation and electron- and light-emitting properties of 8-quinolinol copper(II)–, palladi-

[a] Dr. M. Shirakawa, Dr. N. Fujita, T. Tani, Prof. S. Shinkai
Department of Chemistry & Biochemistry
Graduate School of Engineering
Kyushu University
744 Moto-oka, Nishi-ku, Fukuoka 819-0395 (Japan)
Fax: (+81) 92-802-2820
E-mail: seijitcm@mbox.nc.kyushu-u.ac.jp

[b] Prof. K. Kaneko
HVEM Laboratory, Kyushu University
744 Moto-oka, Nishi-ku, Fukuoka 819-0395 (Japan)

[c] M. Ojima, Prof. A. Fujii, Prof. M. Ozaki
Division of Electrical, Electronic, and Information Engineering,
Graduate School of Engineering
Osaka University Suita
Osaka 565-0871 (Japan)

[d] Prof. S. Shinkai
Center for Future Chemistry, Kyushu University
744 Moto-oka, Nishi-ku, Fukuoka 819-0395 (Japan)

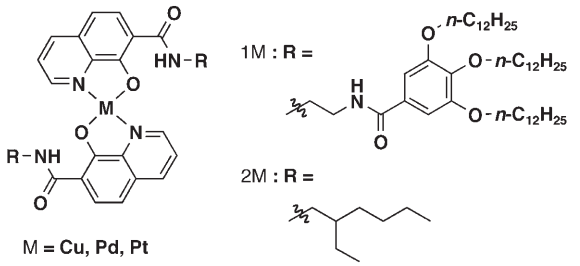

um(II)–, and platinum(II)–chelate derivatives (**1M**) bearing 3,4,5-tris(*n*-dodecyloxy)benzoylamide substituents.[13] We expected that their square-planar chelate structures would be of great advantage to gel formation because of their strong π–π interactions, which are one of the main driving forces for gelation.[14] In addition, it is known that introduction of 3,4,5-tris(alkoxy)phenyl substituents into a π-conjugated planar molecule is favorable for self-assembly into a columnar-stacking structure to give highly ordered structures such as liquid crystals and gels.[15] It is considered that the gel fiber formed should be applicable as an effective electron- and light-emitting nanomaterial, because of exciton delocalization along the fiber network.[16] Furthermore, we can expect that the three kinds of gelators designed would give similarly shaped nanofibers because their coordination geometry is the same, whereas the properties of these fibrous structures could be controlled by choosing the central metal (Figure 1). To clarify the gelation effect, we also designed nongelling reference compounds **2M**, which have 2-ethylhexyl moieties as solubilizing substituents.

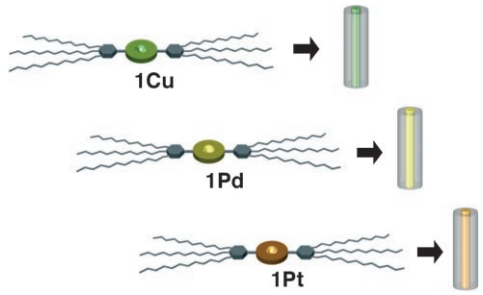

Figure 1. Schematic representation of the **1M** nanofibers that have different electronic states depending on the central metals.

Results and Discussion

Gelation properties of 1M: The gelation properties of the 8-quinolinol/metal(II)–chelate derivatives **1M** were evaluated in various organic solvents by the "stable to inversion of a test tube" method. It is seen from Table 1 that **1Cu**, **1Pd**, and **1Pt** can gelate 18, 19, and 18 solvents, among 25 candidates, respectively, such as, benzene, hexane, 1-butanol, 1,4-dioxane, and so on. Additionally, **1M** derivatives show a very low critical gelation concentration (CGC), 1.0 mg mL^{-1} (ca. 0.5 mM). These results indicate that **1M** derivatives act as versatile gelators for polar solvents, as well as, for nonpolar ones. It is considered, therefore, that such a good gelation ability of **1M** arises from the cooperative action of three different intermolecular interactions, that is, the π–π interaction among the chelate moieties, the hydrogen-bonding interaction among the amide groups, and the van der Waals interaction among the long alkyl chains, that principally exert their power in different environments.

Table 1. Gelation properties of **1M** at 25 °C.[a,b]

Entry	Solvent	1Cu	1Pd	1Pt
1	hexane	G (1)	G (1)	G (1)
2	octane	G (1)	G (1)	G (1)
3	decane	G (1)	G (1)	G (1)
4	cyclohexane	G (1)	G (1)	G (1)
5	methylcyclohexane	G (1)	G (1)	G (1)
6	decalin	G (1)	G (1)	G (1)
7	benzene	G (1)	G (1)	G (1)
8	toluene	G (1)	G (1)	G (1)
9	*p*-xylene	G (1)	G (1)	G (1)
10	pyridine	S	G (10)	S
11	anisole	G (1)	G (1)	G (1)
12	methanol	P	P	P
13	ethanol	G (1)	P	P
14	2-propanol	G (10)	G (10)	G (10)
15	1-butanol	G (1)	G (1)	G (1)
16	acetone	G (1)	G (1)	G (1)
17	THF	G (10)	G (2)	G (5)
18	acetonitrile	P	P	P
19	ethyl acetate	G (1)	G (1)	G (1)
20	1,4-dioxane	G (1)	G (1)	G (1)
21	DMF	P	G (10)	G (5)
22	DMSO	P	P	P
23	dichloromethane	G(10)	G(10)	G(10)
24	chloroform	S	S	S
25	TCE	S	S	S

[a] G: gel; P: precipitate; and S: solution. [b] The critical gelation concentrations [mg mL^{-1}] of gelators are shown in the parentheses.

Electron microscope measurements: The morphology of the **1M** gel fibers was investigated by using a scanning electron microscope (SEM) and a transmission electron microscope (TEM). As shown in Figure 2, we could observe well-developed network structures characteristic of low-molecular-weight organogels, the approximate diameters and the length of the fibrous aggregate of the **1M**+*p*-xylene gels being 10–50 nm and several μm, respectively. We also confirmed the creation of similar fibrous structures in gels prepared from other gelling solvents. It is worth mentioning that the morphology of the fibers prepared from the three gelators, which have different central metal atoms, is almost the same. This result implies that it is possible to create nanomaterials that have the same shape: in other words, the different properties, if they exist, are attributable to the difference in the central metals. This subject is discussed in more detail in a later section.

UV/Vis absorption and FTIR spectroscopic analyses: To obtain insight into the aggregation mode of the chelate moieties and the amide groups in the gel tissue, we measured UV/Vis absorption spectra and FTIR spectra comparing the **1M**+*p*-xylene gels with the **1M**+1,1,2,2-tetrachloroethane (TCE) solutions. 8-Quinolinol/metal(II)–chelate derivatives

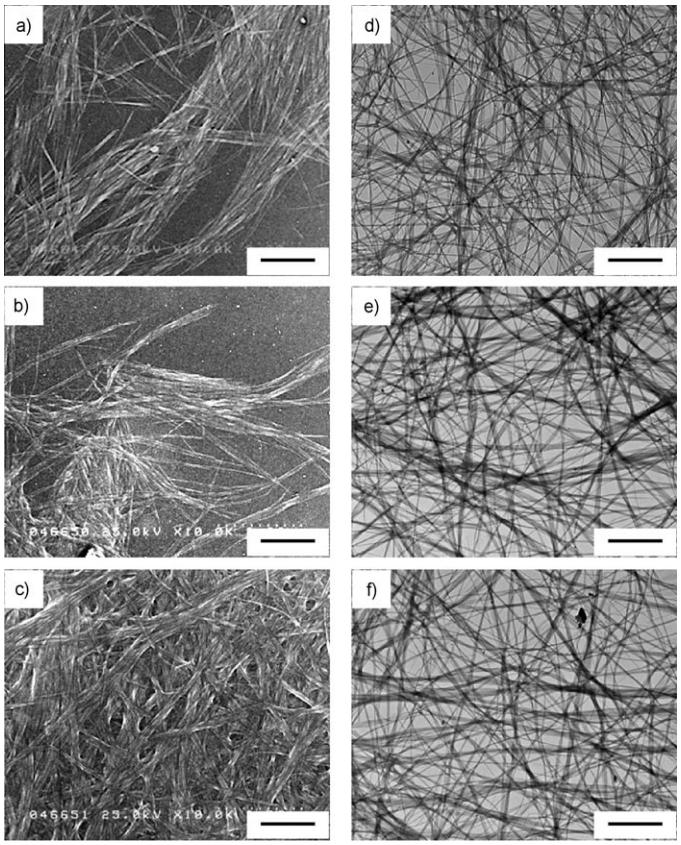

Figure 2. SEM (left) and TEM (right) images of the **1Cu** (top), **1Pd** (middle), and **1Pt**+*p*-xylene (bottom) gels: a–c) [**1M**] = 5 mg mL^{-1}; d–f), [**1M**] = 1 mg mL^{-1}. The scale bar length is 2 μm.

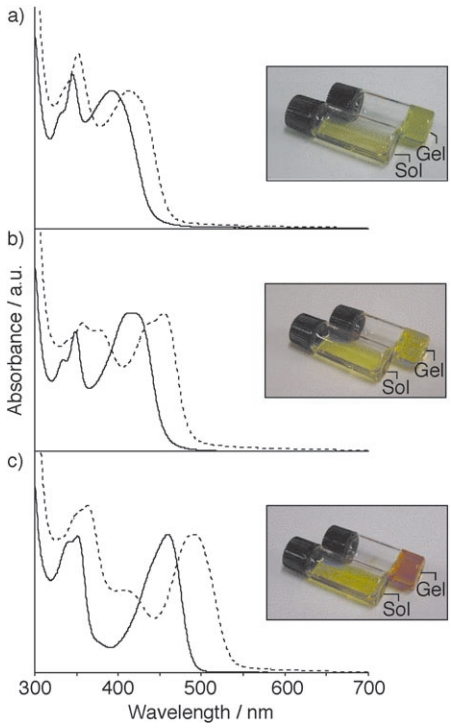

Figure 3. UV/Vis absorption spectra of the **1M**+*p*-xylene gels (– – –) and the **1M**+TCE solutions (——): [**1M**] = 10 mg mL^{-1}; a) [**1Cu**], b) [**1Pd**], and c) **1Pt**. Photographs show the **1M**+*p*-xylene gels and their heated solutions.

have two characteristic absorption bands in the UV/Vis region. One is a ligand-centered π–π transition, which is observed around 350 nm, and the other is a singlet intraligand charge-transfer (^{1}ILCT) transition, which is observed between 380 and 500 nm depending on the central metal. As shown in Figure 3, these two peaks of **1M** are shifted to longer wavelengths in the gel phase compared to those in the solution phase (**1Cu**: λ_{max} = 346→352 (π–π) and 392→413 nm (^{1}ILCT), **1Pd**: λ_{max} = 349→358 (π–π) and 417→455 nm (^{1}ILCT), **1Pt**: λ_{max} = 352→363 (π–π) and 460→491 nm (^{1}ILCT)). These shifts indicate that 8-quinolinol/metal(II)–chelate moieties in the **1M**+*p*-xylene gel tissues tend to adopt a *J*-aggregation mode.[17] Furthermore, these *J* aggregates cause the unique thermochromism in relation to a sol–gel transition phenomenon, especially in the case of **1Pt** (Figure 3c). The color of a heated solution was yellow, whilst that of a cooled gel was orange. We also measured UV/Vis absorption spectra of the **1M**+*n*-decane, 1,4-dioxane, and 1-butanol gels. The spectral patterns were almost the same as that of the *p*-xylene gel, indicating that the aggregation mode of **1M** in the gel phase is scarcely affected by solvents. Meanwhile, formation of the hydrogen bonds among the amide groups is easily discussed by the data obtained from the FTIR measurements. The C=O stretching bands appearing in the gel phase were observed to shift to shorter wavenumbers by 7–10 cm^{-1} compared to those bands appearing in the solution phase, supporting the formation of the intermolecular hydrogen bonds (Figure 4). From these results, 8-quinolinol/metal(II)–chelate-based gelators **1M** self-assemble not only by the van der Waals interaction among the dense long alkyl chains, but also by the π–π interaction among the chelate moieties and hydrogen-bond interaction among the amide groups.

Powder X-ray diffraction: We performed powder X-ray diffraction (XRD) analysis to determine the packing structure of the gelators in detail. Powder XRD analysis of the xerogel prepared from the **1Pt**+benzene gel shows two strong peaks at $2\theta = 2.1°$ (42 Å) and 3.4° (26 Å), which should be assigned to the (1 0 0) diffraction and the (0 1 0) diffraction peaks, respectively (Figure 5). Taking a typical stacking distance of $h \approx 4.5$ Å between two closely packed 3,4,5-tris-(alkoxy)phenyl substituents in the column and a density of $\rho = 1.3$ g cm^{-3} into consideration,[18] we could calculate $Z = 2$, that is, two molecules per unit cell. Therefore, a packing structure shown in Figure 6b is proposed as the most likely aggregation model. The distance of the intercolumnar separation (42 Å) is shorter than the molecular length of **1M** (ca. 52 Å). This result implies that the molecules in the gel tissue are stacked in a tilted fashion along the *c* axis (Figure 6c). As clearly seen in Figure 6d, these π–π stacked structures along the *c* axis were visually confirmed by high-

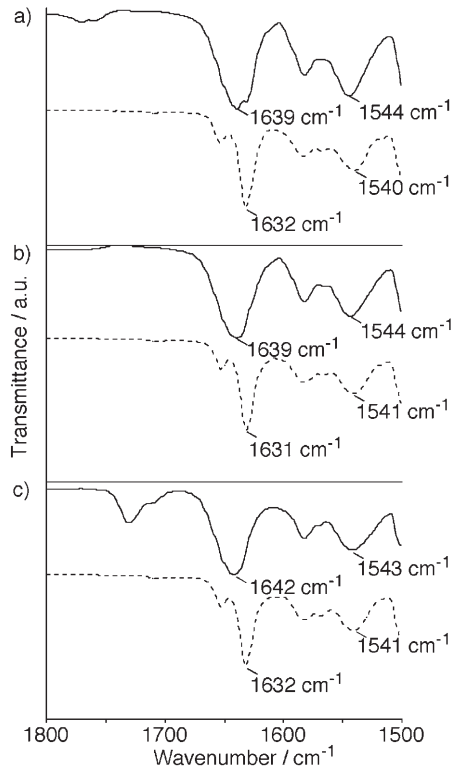

Figure 4. FTIR spectra of the **1M**+*p*-xylene gels (– – –) and the **1M**+TCE solutions (——): [**1M**] = 5 mg mL^{-1}; a) [**1Cu**], b) [**1Pd**], and c) **1Pt**.

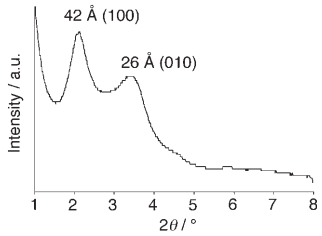

Figure 5. A powder XRD diagram of the xerogel prepared from the **1Pt**+benzene gel: [**1Pt**] = 200 mg mL^{-1}.

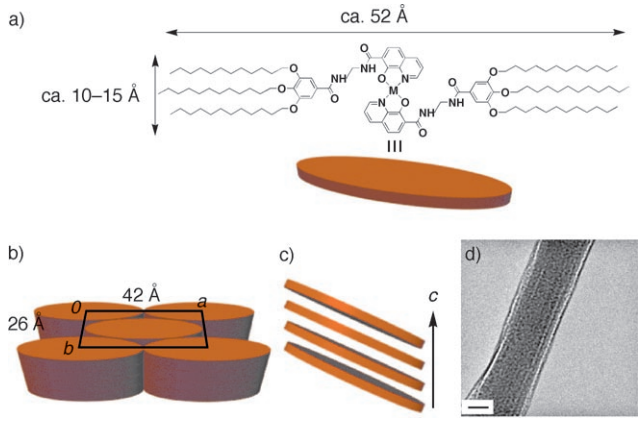

Figure 6. a) Molecular scales of **1M**; b) proposed packing model of **1M** in the gel tissues; c) tilted arrangement of **1M** along the *c* axis, and d) an HRTEM image of the **1Pt**+*p*-xylene gel: [**1Pt**] = 2.0 mg mL^{-1}. The scale bar length is 20 nm.

resolution TEM (HRTEM) as strong stripe contrasts parallel to the axis along the length of the fiber.

Differential pulse voltammetry (DPV) measurements: To compare the electronic state of each metal–chelate derivative, we estimated the electrochemical potential, which is one of the most essential parameters to determine the performance of materials composed of metal–chelate derivatives, by measuring solutions of the nongelling reference compounds **2M** in benzonitrile by DPV analysis (tetrabutylammonium perchlorate: 100 mM; reference electrode: Ag/Ag$^+$; counter electrode: Pt wire; scan rate: 50 mV s^{-1}). The voltammograms obtained for **2M** apparently show different reduction and oxidation potentials depending on the central metals (Figure 7): **2Cu** has a relatively low oxidation potential (990 mV versus Ag/Ag$^+$) and a high reduction potential (−980 mV versus Ag/Ag$^+$), **2Pd** has a relatively high oxidation potential (1190 mV versus Ag/Ag$^+$) and a low reduction potential (−1720 mV versus Ag/Ag$^+$), and **2Pt** has relatively low oxidation (1000 mV versus Ag/Ag$^+$) and reduction potentials (−1800 mV versus Ag/Ag$^+$). Taking the idea into consideration that these differences in the redox potentials should be reflected in the electronic properties of each **1M** gel fiber, we carried out the following experiments.

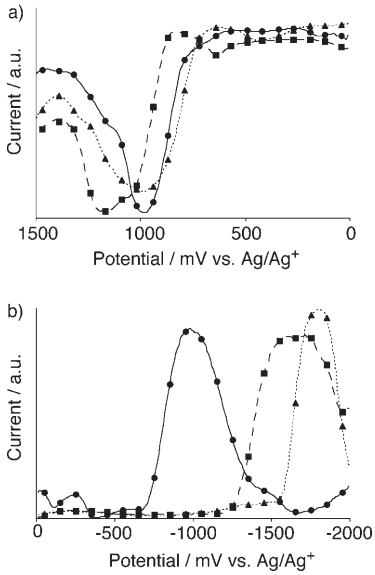

Figure 7. DPV diagrams of the **2M**+benzonitrile solutions; [**2M**] = 10 mM, **2Cu** (●), **2Pd** (■), and **2Pt** (▲); a) Oxidations and b) Reductions.

Field-emission properties of the 1M gel fibers: Field emission of inorganic nanostructures and carbon nanotubes has been reported for many years.[19,20] Meanwhile, it has been confirmed in the last five years that several organic nanostructures also work as effective field-emission materials.[21] As a field emitter, a needle-like shape and semiconducting properties are required. Considering that the **1M** gel fibers can fulfil both requirements, we expect that they would show field-emission properties. Field-emission measure-

ments were carried out with the cast-film of the **1M** gel fiber on an ITO (indium titanium oxide) electrode. Figure 8 shows typical plots of the field-emission current density J versus the applied electric field E of the **1M** cast-films. The

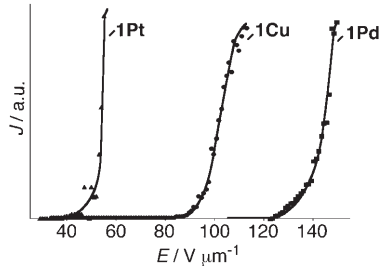

Figure 8. Field-emission J–E curves of the **1M** nanofibers, **1Cu** (●), **1Pd** (■), and **1Pt** (▲).

1Cu, **1Pd**, and **1Pt** cast-films exhibit turn-on field values of approximately 90, 125, and 40 $V\,\mu m^{-1}$, respectively. Although these values are higher than those of other inorganic and organic field-emission materials reported earlier,[12,19–21] the gel fibers have the advantage over other materials in that they are easily prepared by a spontaneous self-assembling process in solution. Furthermore, the turn-on field values of **1M** are clearly different depending on the central metals. As confirmed above, the shapes of the gel fibers prepared from **1M** are almost the same, because their self-assembling properties are mainly dominated by the organic ligand moieties and the three kinds of central metals have the same coordination geometry. The above-mentioned results therefore imply that the field-emission performances of nanofibers with the same shape are easily controlled by changing the central metals. Generally speaking, it is very difficult, especially in the nanoscale region, to control the turn-on field value by molecular design. In this context, the present metallogel system has a unique character.

Phosphorescence spectra of 1Pt: Next, we focus upon the influence of the gel formation on phosphorescence properties of **1Pt**. It is known that 8-quinolinol/platinum(II)–chelate derivatives show red phosphorescence around 600–650 nm, which is emitted from the triplet ligand-centered transitions ($^3\pi$–π or ^{3}ILCT).[22] We observed light orange phosphorescence appearing at 620 nm from the **1Pt**+TCE solution, whereas red phosphorescence appeared at 650 nm from the **1Pt**+*p*-xylene gel under UV light (Figure 9). This color change originates from J aggregation of the chelate moieties as confirmed by the UV/Vis absorption spectra and the powder XRD analysis. Moreover, this red phosphorescence is emitted from a nanoscale fibrous structure, which is directly observable by confocal laser scanning microscopy (CLSM) (Figure 9c).

Inhibition efficiency of dioxygen quenching: Phosphorescent materials composed of metal–chelate derivatives have gained much interest due to their advantages of long-lived

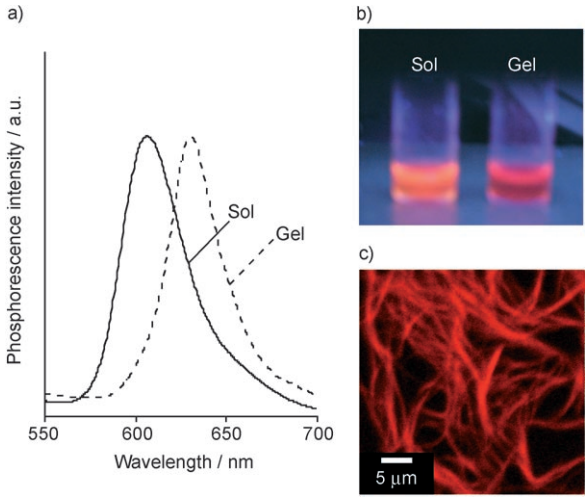

Figure 9. a) Phosphorescence spectra of the **1Pt**+*p*-xylene gel (– – –) and the **1Pt**+TCE solution (——): [**1Pt**] = 2.0 $mg\,mL^{-1}$, excited at 490 nm for the gel and at 460 nm for the solution. b) A photograph of the **1Pt** gel and solution under UV light (365 nm). c) A CLSM image of the **1Pt**+*p*-xylene gel: [**1Pt**] = 2.0 $mg\,mL^{-1}$.

luminescence and high luminescence quantum yield for various applications such as electroluminescent displays,[23] sensors,[24] photovoltaic devices,[25] and photocatalysts.[26] Considering the practical utilization of phosphorescent materials, the most essential, but difficult, problem is how to avoid the dioxygen quenching of their excited triplet states. One of the successful methods in aqueous solution is to utilize micellar functions in which the collisional deactivation of excited triplet states can be minimized by solute partitioning to the micellar phase.[27] Meanwhile, low-molecular-weight gel tissues are produced by microphase (or nanophase) separation of gelator molecules and solvent molecules, in which the gelator phase is well segregated from the solvent phase that contains dioxygen. In addition, the gelator assemblies have a crystal-like nature favorable to segregation, being different from the dynamic nature characteristic of the micellar systems. Considering that the phosphorescent chelate moieties are located inside the **1Pt** gel fibers, deactivation of excited triplet states by collision with dioxygen molecules could be effectively inhibited. To estimate the inhibition efficiency of dioxygen quenching ($E_{vs.O_2}$) we conducted the following experiments. Phosphorescence spectra of **1Pt** and **2Pt** were measured under an argon atmosphere or a dioxygen-saturated atmosphere in the gel phase or in the solution phase,[28] for which we defined $E_{vs.O_2}$ as $PI_{dioxygen}/PI_{argon} \times 100$ under each measurement condition.[29] The experimental results are summarized in Figure 10. We found that the $E_{vs.O_2}$ values of **1Pt** are larger than those of **2Pt** in all gelling solvents, such as *p*-xylene, 1,4-dioxane, and 1-butanol. On the other hand, the $E_{vs.O_2}$ values of **1Pt** and **2Pt** are almost the same in the nongelling solvent TCE. These results support the view that the increase of the $E_{vs.O_2}$ is not due to the difference in the peripheral substituent structure, but due to the molecular assembling effect in the gel phase. In other

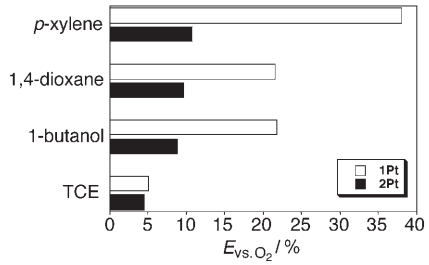

Figure 10. $E_{vs.\,O_2}$ values of **1Pt** (white) and **2Pt** (black) for four kinds of solvents: [**1Pt**] = [**2Pt**] = 1 mM.

words, one can regard that the gel phase is capable of protecting the chromophore moiety from dioxygen quenching.

Conclusion

We have demonstrated that 3,4,5-tris(*n*-dodecyloxy)benzoylamide substituents appended 8-qinolinol/metal(II)–chelates **1M** act as highly efficient gelators for various organic solvents. This gelation capability is attributed to the strong π–π interactions of chelate moieties as well as the hydrogen-bond interactions among the amide groups. As confirmed by the field-emission measurements, the electronic properties of the three kinds of gel fibers obtained are evidently different depending on the central metals although their shapes are almost the same. In the case of **1Pt**, the π–π interaction of the chelate moiety results in thermo- and solvatochromism of visible color and a color change in the phosphorescence emission in response to a sol–gel phase transition. Furthermore, it was shown that dioxygen quenching of the excited triplet states is efficiently inhibited in the gel phase. These findings consistently indicate that introduction of metal chelates into the low-molecular-weight gel system is one of the most effective strategies to obtain a wide variety of photo- and electrochemical nanomaterials.

Experimental Section

All starting materials and solvents were purchased from Aldrich, TCI, Kishida Chemical, or Wako, and were used as received. ^{1}H NMR spectra were recorded by using Bruker AC-250 PC and DMX 600 spectrometers. Chemical shifts are reported in ppm downfield from tetramethylsilane (TMS) as the internal standard. FTIR spectra were obtained by using a Perkin–Elmer instrument Spectrum One FTIR spectrometer. Mass spectral data were obtained by using a Perseptive Voyager RP MALDI-TOF mass spectrometer. UV/Vis and phosphorescence spectra were recorded by using a Shimadzu UV-2500PC spectrometer and a Perkin–Elmer LS 55 luminescence spectrometer, respectively. DPV measurements were performed by using a BAS 100B/W (CV-50W) instrument.

Gelation test: The gelator and the solvent were put in a septum-capped test tube and heated until the solid was dissolved. The sample vial was cooled in air to 25 °C, then left for 1 h at this temperature. The state of the materials was evaluated by the "stable to inversion of a test tube" method.

SEM and TEM measurements: For SEM observations, a piece of the gel was placed on a carbon-coated copper grid and was dried in vacuo for 12 h at RT. Then, the obtained sample was shielded by Pt and was examined with a Hitachi S-5000 scanning electron microscope. The accelerating voltage was 25 kV. For TEM observations, a carbon-coated copper grid was immersed in the gel and dried for 12 h under reduced pressure. The grid was examined with a Hitachi H-600 transmission electron microscope, operating at 120 kV.

Powder X-ray diffraction: The gel was prepared in a sample tube and was frozen by using liquid nitrogen. The frozen specimen was evaporated by using a vacuum pump for 1 day at RT. The obtained xerogel was put in a capillary ($\Phi = 2.0$ mm). An X-ray diffraction pattern was recorded on an imaging plate by using Cu radiation ($\lambda = 1.54178$ Å).

Confocal laser scanning microscopy (CLSM) measurements: The **1Pt**+ *p*-xylene gel was placed on a glass plate and was observed with a BIO-RAD Radiance 2000 AGR3 microscope. The excitation wavelength was 514 nm (argon laser with reflector turret).

Field-emission measurements: Field-emission measurements were carried out in a high-vacuum chamber under about 10^{-7} Torr pressure. We used a tungsten probe with a diameter of 500 μm as an anode.[30] The cross-sectional area of the anode was 1.96×10^{-7} m^2. Field-emission current density and electric field characteristics were measured for a constant distance (10 μm) between the anode and the **1M** nanofibers.

Syntheses of 8-quinolinol/metal(II)-chelate-based gelators and nongelling reference compounds: Compounds **1M** and **2M** were synthesized according to Scheme 1 and identified by MALDI-TOF mass spectrometry, ^{1}H NMR, FTIR, and UV/Vis absorption spectra, and elemental analysis. Compound **5** was prepared as described earlier.[13] 3,4,5-Trihydroxybenzoic acid methyl ester was converted into its ether (**3**) by the reaction with 1-bromododecane. Subsequent hydrolysis of the ester groups with NaOH yielded **4**. The coupling reaction of **4** with ethylenediamine gave **5**.

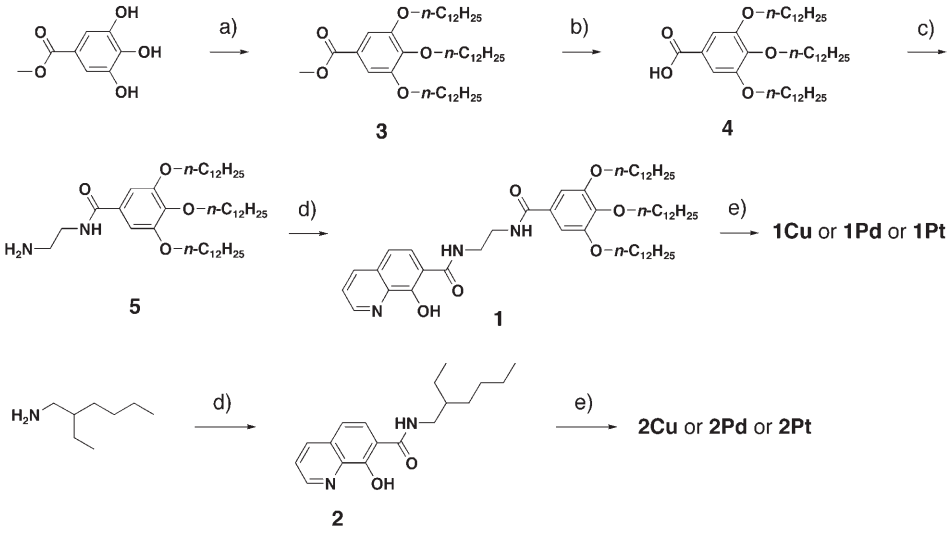

Scheme 1. Syntheses of **1M** and **2M**: a) *n*-$C_{12}H_{25}Br$, K_2CO_3, DMF, 60 °C; b) NaOH, 1,4-dioxane, H_2O, reflux; c) Ethylenediamine, BOP reagent, THF, reflux; d) 8-Quinolinol-7-carboxylic acid, BOP reagent, TEA, THF, reflux; e) $Cu(OAc)_2$, $CHCl_3$, MeOH, 25 °C for **1Cu** and **2Cu**; $Pd(OAc)_2$, $CHCl_3$, MeOH, 25 °C for **1Pd** and **2Pd**; K_2PtCl_4, NaOH, H_2O, 2-propanol, reflux, for **1Pt** and **2Pt**.

Preparation of 1: Compound **5** (2.0 g, 4.1 mmol) was dissolved in THF (30 mL). BOP reagent (1.9 g, 4.2 mmol), triethylamine (430 mg, 4.2 mmol), and 8-hydroxyquinoline-7-carboxylic acid (790 mg, 4.2 mmol) were added to the solution and the resultant mixture was refluxed for 3 h. After cooling the mixture to RT, the solution was concentrated under reduced pressure. The resultant residue was dissolved in $CHCl_3$ and was washed with brine three times. The organic layer was dried over anhydrous Na_2CO_3 and concentrated under reduced pressure. The resultant residue was subjected to column chromatography (silica gel, $CHCl_3$/MeOH 20:1 (v/v)) to give **1** in 84% (2.1 g) yield as a white solid. ^{1}H NMR (250 MHz, $CDCl_3$, TMS, RT): δ = 0.84–0.88 (m, 9H), 1.20–1.60 (m, 54H), 1.67–1.88 (m, 6H), 3.67–3.79 (m, 2H), 3.79–3.91 (m, 2H), 3.97 (t, J = 6.5 Hz, 2H), 4.04 (t, J = 6.5 Hz, 4H), 7.07 (s, 2H), 7.37 (d, J = 8.7 Hz, 1H), 7.50–7.60 (m, 2H), 8.14 (d, J = 9.0 Hz, 1H), 8.18 (m, 1H), 8.42–8.48 (m, 1H), 8.86 ppm (m, 1H); MALDI-TOF MS (dithranol): m/z calcd for $[M+H]^+$: 888.68; found: 888.61; elemental analysis calcd (%) for $C_{55}H_{89}N_3O_6$: C 74.36, H 10.10, N 4.73; found: C 74.26, H 10.06, N 4.73.

Preparation of 1Cu: A suspension of $Cu(OAc)_2$ (10.0 mg, 0.055 mmol) in methanol (2 mL) was added to a solution of compound **1** (100 mg, 0.11 mmol) in chloroform (10 mL), and the mixture was stirred at RT for 20 min. The reaction mixture was poured into methanol (100 mL), and the resultant precipitate was collected. The obtained solid was further purified by the recrystallization from the mixed solvent of methanol and ethyl acetate to give **1Cu** in 70% yield (72 mg) as a greenish solid. IR (NaCl): $\tilde{\nu}$ = 3284, 2928, 2855, 1639, 1582, 1544, 1499, 1450, 1386 cm^{-1}; UV/Vis (TCE): λ_{max} = 332, 346, 393 nm; MALDI-TOF MS (dithranol): m/z calcd for $[M+H]^+$: 1837.3; found: 1836.1; elemental analysis calcd (%) for $C_{110}H_{176}CuN_6O_{12}\cdot H_2O$: C 71.18, H 9.67, N 4.53; found: C 71.21, H 9.53, N 4.50.

Preparation of 1Pd: This compound was prepared by a procedure similar to that for the synthesis of compound **1Cu** from **1** and $Pd(OAc)_2$ and **1Pd** was obtained as a yellow solid (yield 76%). ^{1}H NMR (600 MHz, [D$_4$]TCE, TMS, 80 °C): δ = 0.85–0.87 (m, 18H), 1.24–1.28 (m, 96H), 1.41–1.43 (m, 12H), 1.67 (m, 4H), 1.74 (m, 8H), 3.71 (m, 4H), 3.83 (m, 4H), 3.89 (t, J = 6.5 Hz, 4H), 3.96 (t, J = 6.4 Hz, 8H), 7.02 (s, 4H), 7.07 (d, J = 8.5 Hz, 2H), 7.27 (br, 2H), 7.53 (m, 2H), 8.25 (d, J = 8.5 Hz, 2H), 8.29 (m, 4H), 9.44 ppm (t, J = 5.8 Hz, 2H); IR (NaCl): $\tilde{\nu}$ = 3303, 2928, 2855, 1639, 1582, 1544, 1500, 1448, 1375 cm^{-1}; UV/Vis (TCE): λ_{max} = 334, 349, 418 nm; MALDI-TOF MS (dithranol): m/z calcd for $[M+H]^+$: 1880.2; found: 1879.5; elemental analysis calcd (%) for $C_{110}H_{176}N_6O_{12}Pd\cdot H_2O$: C 69.57, H 9.45, N 4.43; found: C 69.33, H 9.15, N 4.46.

Preparation of 1Pt: A solution of K_2PtCl_4 (23 mg, 55 μmol) in aqueous NaOH (pH 10, 1 mL) was added to a suspension of compound **1** (100 mg, 0.11 mmol) in 2-propanol (30 mL). The reaction mixture was refluxed for 20 h. After cooling the mixture to RT, the solution was concentrated under reduced pressure. The resultant residue was subjected to column chromatography (silica gel, $CHCl_3$/MeOH 20:1 (v/v)) to give **1Pt** in 40% (44 mg) yield as an orange solid. ^{1}H NMR (600 MHz, [D$_4$]TCE, TMS, 80 °C): δ = 0.86–0.88 (m, 18H), 1.25–1.28 (m, 96H), 1.39–1.43 (m, 12H), 1.66 (m, 4H), 1.73 (m, 8H), 3.74 (m, 4H), 3.87 (m, 4H), 3.89 (t, J = 6.5 Hz, 4H), 3.95 (t, J = 6.5 Hz, 8H), 7.01 (s, 4H), 7.06 (d, J = 8.5 Hz, 2H), 7.22 (br, 2H), 7.55 (dd, J = 8.3, 5.0 Hz, 2H), 8.24 (d, J = 8.5 Hz, 2H), 8.33 (d, J = 8.3 Hz, 2H), 8.62 (d, J = 4.8 Hz, 2H), 9.36 ppm (t, J = 5.9 Hz, 2H); IR (NaCl): $\tilde{\nu}$ = 3322, 2928, 2855, 1642, 1583, 1543, 1502, 1449 cm^{-1}; UV/Vis (TCE): λ_{max} = 341, 351, 460 nm; MALDI-TOF MS (dithranol) m/z calcd for $[M+H]^+$: 1969.30; found: 1969.54; elemental analysis calcd (%) for $C_{110}H_{176}N_6O_{12}Pt\cdot 0.50\ H_2O$: C 66.77, H 9.02, N 4.25; found: C 66.70, H 8.96, N 4.25.

Preparation of 2: 2-Ethylhexylamine (360 g, 2.8 mmol) was dissolved in THF (30 mL). BOP reagent (1.9 g, 4.2 mmol), triethylamine (420 mg, 4.2 mmol), and 8-hydroxyquinoline-7-carboxylic acid (790 mg, 4.2 mmol) were added to the solution and the mixture was refluxed for 3 h. After cooling the mixture to RT, the solution was concentrated under reduced pressure. The resultant residue was dissolved in $CHCl_3$ and was washed with brine three times. The organic layer was dried over anhydrous Na_2CO_3 and concentrated under reduced pressure. The resultant residue was subjected to column chromatography (silica gel, $CHCl_3$/MeOH 10:1 (v/v)) to give **2** in 80% (670 mg) yield as a white solid; ^{1}H NMR (250 MHz, $CDCl_3$, TMS, RT): δ = 0.87–0.98 (m, 6H), 1.20–1.50 (m, 8H), 1.60–1.70 (m, 1H), 3.50 (t, J = 5.3 Hz, 2H), 7.34 (d, J = 8.9 Hz, 1H), 7.48 (dd, J = 8.2, 4.2 Hz, 1H), 7.99 (br, 1H), 8.13–8.18 (m, 2H), 8.83 ppm (d, J = 3.3 Hz, 1H); MALDI-TOF MS (dithranol): m/z calcd for $[M+H]^+$: 301.18; found: 303.84; elemental analysis calcd (%) for $C_{18}H_{24}N_2O_2$: C 71.97, H 8.05, N 9.33; found: C 71.76, H 8.04, N 9.26.

Preparation of 2Cu: This compound was prepared by a procedure similar to that for the synthesis of compound **1Cu** from **2** and $Cu(OAc)_2$, and **2Cu** was obtained as an greenish solid (yield 85%). IR (NaCl): $\tilde{\nu}$ = 3299, 2930, 1638, 1547, 1499, 1385 cm^{-1}; UV/Vis (TCE): λ_{max} = 331, 345, 398 nm; MALDI-TOF MS (dithranol): m/z calcd for $[M+Na]^+$: 682.3; found: 684.3; elemental analysis calcd (%) for $C_{36}H_{46}CuN_4O_4$: C 65.28, H 7.00, N 8.46; found: C 65.35, H 6.96, N 8.41.

Preparation of 2Pd: This compound was prepared by a procedure similar to that for the synthesis of compound **1Cu** from **2** and $Pd(OAc)_2$, and **2Pd** was obtained as a yellow solid (yield 72%). ^{1}H NMR (600 MHz, [D$_4$]TCE, TMS, 80 °C): δ = 0.89 (t, J = 6.9 Hz, 6H), 1.00 (t, J = 7.0 Hz, 6H), 1.31–1.34 (m, 4H), 1.40–1.45 (m, 8H), 1.50–1.53 (m, 4H), 1.62–1.65 (m, 2H), 3.50 (m, 4H), 7.07 (d, J = 8.4 Hz, 2H), 7.45 (m, 2H), 8.31 (d, J = 8.3 Hz, 2H), 8.34–36 (m, 4H), 9.04 ppm (br, 2H); IR (NaCl): $\tilde{\nu}$ = 3686, 2929, 1637, 1603, 1546, 1501, 1448, 1374 cm^{-1}; UV/Vis (TCE): λ_{max} = 334, 349, 425 nm; MALDI-TOF MS (dithranol): m/z calcd for $[M+H]^+$: 703.2; found: 703.9; elemental analysis calcd (%) for $C_{36}H_{46}N_4O_4Pd$: C 61.31, H 6.57, N 7.94; found: C 61.29, H 6.58, N 7.90.

Preparation of 2Pt: This compound was prepared by a procedure similar to that for the synthesis of compound **1Pt** from **2** and K_2PtCl_4, and **2Pt** was obtained as an orange solid (yield 4%). ^{1}H NMR (600 MHz, [D$_4$]TCE, TMS, 80 °C): δ = 0.90 (t, J = 7.1 Hz, 6H), 1.01 (t, J = 7.3 Hz, 6H), 1.20–1.80 (m, 18H), 3.53 (m, 4H), 7.10 (d, J = 8.5 Hz, 2H), 7.45 (m, 2H), 8.29 (d, J = 8.4 Hz, 2H), 8.39 (d, J = 8.3 Hz, 2H), 8.64 (m, 2H), 8.90 ppm (m, 2H); IR (NaCl): $\tilde{\nu}$ = 3686, 3341, 2929, 1639, 1603, 1547, 1502, 1449, 1375 cm^{-1}; UV/Vis (TCE): λ_{max} = 342, 351, 464 nm; MALDI-TOF MS (dithranol): m/z calcd for $[M+H]^+$: 794.32; found: 793.36; elemental analysis calcd (%) for $C_{36}H_{46}N_4O_4Pt$: C 54.47, H 5.84, N 7.06; found: C 54.29, H 5.84, N 7.06.

Acknowledgements

This work was partially supported by the Ministry of Education, Culture, Sports, Science, and Technology (Japan) through Grants-in-Aid (No. 16750122, 15105004,and 18033040) and through the 21st Century COE Program, "Functional Innovation of Molecular Informatics". A JSPS fellowship for M.S. is also acknowledged.

[1] For the recent reviews: a) P. Terech, R. G. Weiss, *Chem. Rev.* **1997**, *97*, 3133–3160; b) D. J. Abdallah, R. G. Weiss, *Adv. Mater.* **2000**, *12*, 1237–1247; c) J. H. van Esch, B. L. Feringa, *Angew. Chem.* **2000**, *112*, 2351–2354; *Angew. Chem. Int. Ed.* **2000**, *39*, 2263–2266; d) S. Shinkai, K. Murata, *J. Mater. Chem.* **1998**, *8*, 485–495.

[2] For the recent reviews: a) F. J. M. Hoeben, P. Jonkheijm, E. W. Meijer, A. P. H. J. Schenning, *Chem. Rev.* **2005**, *105*, 1491–1546; b) A. P. H. J. Schenning, E. W. Meijer, *Chem. Commun.* **2005**, 3245–3258; c) T. Ishi-i, S. Shinkai, *Top. Curr. Chem.* **2005**, *258*, 119–160.

[3] K. Sugiyasu, N. Fujita, S. Shinkai, *J. Synth. Org. Chem. Jpn.* **2005**, *63*, 359–369.

[4] F. Fages, *Angew. Chem.* **2006**, *118*, 1710–1712; *Angew. Chem. Int. Ed.* **2006**, *45*, 1680–1682.

[5] a) S.-i. Kawano, N. Fujita, S. Shinkai, *J. Am. Chem. Soc.* **2004**, *126*, 8592–8593; b) K. Tsuchiya, Y. Orihara, Y. Kondo, N. Yoshio, T. Ohkubo, H. Sakai, M. Abe, *J. Am. Chem. Soc.* **2002**, *126*, 12282–12283.

[6] a) B. Xing, M.-F. Choi, B. Xu, *Chem. Eur. J.* **2002**, *8*, 5028–5032; b) J. F. Miravet, B. Escuder, *Chem. Commun.* **2005**, 5796–5798.

[7] a) J. B. Beck, S. J. Rowan, *J. Am. Chem. Soc.* **2003**, *125*, 13922–13923; b) A. Kishimura, T. Yamashita, T. Aida, *J. Am. Chem. Soc.* **2005**, *127*, 179–183.
[8] a) K. Kuroiwa, T. Shibata, A. Takada, N. Nemoto, N. Kimizuka, *J. Am. Chem. Soc.* **2004**, *126*, 2016–2021; b) O. Roubeau, A. Colin, V. Schmitt, R. Clérac, *Angew. Chem.* **2004**, *116*, 3345–3348; *Angew. Chem. Int. Ed.* **2004**, *43*, 3283–3286.
[9] M. Shirakawa, N. Fujita, S. Shinkai, *J. Am. Chem. Soc.* **2005**, *127*, 4164–4165.
[10] a) M. Takeuchi, S. Tanaka, S. Shinkai, *Chem. Commun.* **2005**, 5539–5541; b) T. Kishida, N. Fujita, K. Sada, S. Shinkai, *J. Am. Chem. Soc.* **2005**, *127*, 7298–7299; c) T. Kishida, N. Fujita, O. Hirata, S. Shinkai, *Org. Biomol. Chem.* **2006**, *4*, 1902–1909; d) T. Naota, H. Koori, *J. Am. Chem. Soc.* **2005**, *127*, 9324–9325.
[11] C. W. Tang, S. A. VanSlyke, *Appl. Phys. Lett.* **1987**, *51*, 913–915.
[12] J.-J. Chiu, C.-C. Kei, T.-P. Perng, W.-S. Wang, *Adv. Mater.* **2003**, *15*, 1361–1364.
[13] Preliminary communication: M. Shirakawa, N. Fujita, T. Tani, K. Kaneko, S. Shinkai, *Chem. Commun.* **2005**, 4149–4151.
[14] a) F. S. Schoonbeek, J. H. van Esch, B. Wegewijs, D. B. A. Rep, M. P. de Haas, T. M. Klapwijk, R. M. Kellogg, B. L. Feringa, *Angew. Chem.* **1999**, *111*, 1486–1490; *Angew. Chem. Int. Ed.* **1999**, *38*, 1393–1397; b) A. Ajayaghosh, S. J. George, *J. Am. Chem. Soc.* **2001**, *123*, 5148–5149; c) M. Shirakawa, S.-i. Kawano, N. Fujita, K. Sada, S. Shinkai, *J. Org. Chem.* **2003**, *68*, 5037–5044; d) K. Sugiyasu, N. Fujita, S. Shinkai, *Angew. Chem.* **2004**, *116*, 1249–1253; *Angew. Chem. Int. Ed.* **2004**, *43*, 1229–1233; e) J. P. Hill, W. Jin, A. Kosaka, T. Fukushima, H. Ichihara, T. Shimomura, K. Ito, T. Hashizume, N. Ishii, T. Aida, *Science* **2004**, *304*, 1481–1483.
[15] a) J. Barberá, E. Cavero, M. Lehmann, J.-L. Serrano, T. Sierra, J. T. Vázquez, *J. Am. Chem. Soc.* **2003**, *125*, 4527–4533; b) K. Pieterse, A. Lauritsen, A. P. H. J. Schenning, J. A. J. M. Vekemans, E. W. Meijer, *Chem. Eur. J.* **2003**, *9*, 5597–5604; c) M. Hashimoto, S. Ujiie, A. Mori, *Adv. Mater.* **2003**, *15*, 797–800; d) M. Yoshio, T. Mukai, H. Ohno, T. Kato, *J. Am. Chem. Soc.* **2004**, *126*, 994–995; e) M. Fischer, G. Lieser, A. Rapp, I. Schnell, W. Mamdouh, S. De Feyter, F. C. De Schryver, S. Höger, *J. Am. Chem. Soc.* **2004**, *126*, 214–222; f) T. Kitahara, M. Shirakawa, S.-i. Kawano, U. Beginn, N. Fujita, S. Shinkai, *J. Am. Chem. Soc.* **2005**, *127*, 14980–14981; g) P. Mukhopadhyay, Y. Iwashita, M. Shirakawa, S.-i. Kawano, N. Fujita, S. Shinkai, *Angew. Chem.* **2006**, *118*, 1622–1625; *Angew. Chem. Int. Ed.* **2006**, *45*, 1592–1595.
[16] A. Del Guerzo, A. G. L. Olive, J. Reichwagen, H. Hopf, J.-P. Desvergne, *J. Am. Chem. Soc.* **2005**, *127*, 17984–17985.
[17] *J*-Aggregation phenomena were also reported previously for dye systems appended with 3,4,5-tris(*n*-alkoxy)phenyl substituents: a) F. Würthner, C. Thalacker, S. Diele, C. Tschierske, *Chem. Eur. J.* **2001**, *7*, 2245–2253; b) S. Yao, U. Beginn, T. Gress, M. Lysetska, F. Würthner, *J. Am. Chem. Soc.* **2004**, *126*, 8336–8348; c) F. Würthner, Z. Chen, F. J. M. Hoeben, P. Osswald, C.-C. You, P. Jonkheijm, J. van Herrikhuyzen, A. P. H. J. Schenning, P. P. A. M. van der Schoot, E. W. Meijer, E. H. A. Beckers, S. C. J. Meskers, R. A. J. Janssen, *J. Am. Chem. Soc.* **2004**, *126*, 10612–10618.
[18] Powder of **1Pt** was immersed in several calibrating organic solvents. We decided that the approximate density of **1Pt** was the point at which the powder neither floated nor sank.
[19] a) K. W. Wong, X. T. Zhou, F. C. K. Au, H. L. Lai, C. S. Lee, S. T. Lee, *Appl. Phys. Lett.* **1999**, *75*, 2918–2920; b) F. G. Tarntair, C. Y. Wen, L. C. Chen, J.-J. Wu, K. H. Chen, P. F. Kuo, S. W. Chang, Y. F. Chen, W. K. Hong, H. C. Cheng, *Appl. Phys. Lett.* **2000**, *76*, 2630–2632.
[20] a) W. A. de Heer, A. Châtelain, D. Ugarte, *Science* **1995**, *270*, 1179–1180; b) J. M. Bonard, J. P. Salvetat, T. Stöckli, W. A. de Heer, L. Forró, A. Châtelain, *Appl. Phys. Lett.* **1998**, *73*, 918–920; c) S. Fan, M. G. Chapline, N. R. Franklin, T. W. Tombler, A. M. Cassell, H. Dai, *Science*, **1999**, *283*, 512–514.
[21] a) I. Musa, D. A. I. Munindrasdasa, G. A. J. Amaratunga, W. Eccleston, *Nature* **1998**, *395*, 362–365; b) I. Kymissis, A. I. Akinwande, *Appl. Phys. Lett.* **2003**, *82*, 2347–2349; c) H. Gan, H. Liu, Y. Li, Q. Zhao, Y. Li, S. Wang, T. Jiu, N. Wang, X. He, D. Yu, D. Zhu, *J. Am. Chem. Soc.* **2005**, *127*, 12452–12453.
[22] a) R. Ballardini, M. T. Indelli, G. Varani, C. A. Bignozzi, F. Scandola, *Inorg. Chim. Acta* **1978**, *71*, L423–L424; b) R. Ballardini, G. Varani, M. T. Indelli, F. Scandola, *Inorg. Chem.* **1986**, *25*, 3858–3865; c) D. Donges, J. K. Nagle, H. Yersin, *Inorg. Chem.* **1997**, *36*, 3040–3048.
[23] a) M. A. Baldo, D. F. O'Brien, Y. You, A. Shoustikov, S. Sibley, M. E. Thompson, S. R. Forrest, *Nature* **1998**, *395*, 151–154; b) C. Adachi, M. A. Baldo, M. E. Thompson, S. R. Forrest, *J. Appl. Phys.* **2001**, *90*, 5048–5051; c) Y.-Y. Lin, S.-C. Chan, M. C. W. Chan, Y.-J. Hou, N. Zhu, C.-M. Che, Y. Liu, Y. Wang, *Chem. Eur. J.* **2003**, *9*, 1263–1272; d) W. Lu, B.-X. Mi, M. C. W. Chan, Z. Hui, C.-M. Che, N. Zhu, S.-T. Lee, *J. Am. Chem. Soc.* **2003**, *125*, 4958–4971.
[24] a) C. S. Peyratout, T. K. Aldridge, D. K. Crites, D. R. McMillin, *Inorg. Chem.* **1995**, *34*, 4484–4489; b) J. N. Demas, B. A. DeGraff, *Coord. Chem. Rev.* **2001**, *211*, 317–351.
[25] a) M. A. Fox, H.-L. Pan, W. E. Jones, Jr., D. Melamed, *J. Phys. Chem.* **1995**, *99*, 11523–11530; b) A. Islam, H. Sugihara, K. Hara, L. P. Singh, R. Katoh, M. Yanagida, Y. Takahashi, S. Murata, H. Arakawa, G. Fujihashi, *Inorg. Chem.* **2001**, *40*, 5371–5380; c) J. E. McGarrah, Y.-J. Kim, M. Hissler, R. Eisenberg, *Inorg. Chem.* **2001**, *40*, 4510–4511; d) M.-H. Qi, G.-F. Liu, *J. Phys. Chem. B* **2003**, *107*, 7640–7646.
[26] a) D. Zhang, L.-Z. Wu, L. Zhou, X. Han, Q.-Z. Yang, L.-P. Zhang, C.-H. Tung, *J. Am. Chem. Soc.* **2004**, *126*, 3440–3441; b) M. Hissler, J. E. McGarrah, W. B. Connick, D. K. Geiger, S. D. Cummings, R. Eisenberg, *Coord. Chem. Rev.* **2000**, *208*, 115–137.
[27] a) N. J. Turro, K.-C. Liu, M.-F. Chow, P. Lee, *Photochem. Photobiol.* **1978**, *27*, 523–529; b) R. Humphry-Baker, Y. Moroi, M. Grätzel, *Chem. Phys. Lett.* **1978**, *58*, 207–210.
[28] Argon and dioxygen atmospheres were generated by the following procedure. The solvents used for the experiment were purged by argon or dioxygen for one hour. The inside of the optical cell was filled with argon or dioxygen. Contact with air was prevented as much as possible during the experiment.
[29] PI_{dioxygen} and PI_{argon} stand for the phosphorescence intensity of **1Pt** in a dioxygen-saturated or argon atmosphere, respectively.
[30] M. Ojima, S. Hiwatashi, H. Araki, A. Fujii, M. Ozaki, K. Yoshino, *Appl. Phys. Lett.* **2006**, *88*, 053103.

Received: December 18, 2006
Published online: April 3, 2007

